Journal of Materials Chemistry A

Accepted Manuscript

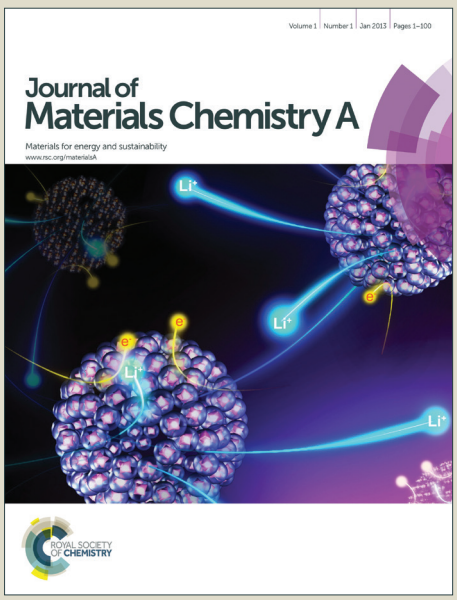

ROYAL SOCIETY OF CHEMISTRY

www.rsc.org/materialsA

Cite this: DOI: 10.1039/c0xx00000x

www.rsc.org/xxxxxx

ARTICLE TYPE

Surface charge tuning of functionalized silica cross-linked micellar nanoparticles encapsulating a Donor-Acceptor dye for Fe (III) sensing

Fangyuan Gai,[a] Tianlei Zhou,[b] Yunling Liu[a] and Qisheng Huo*[a]

Received (in XXX, XXX) Xth XXXXXXXXX 20XX, Accepted Xth XXXXXXXXX 20XX

DOI: 10.1039/b000000x

In this study, a water-soluble Fe^{3+} ratiometric fluorescence sensor was designed and synthesized by encapsulating a Donor-Acceptor (D-A) dye 4-formacyl-triphenylamine (FTA) into silica cross-linked micellar nanoparticles (SCMNPs). The quenching of FTA-encapsulated SCMNPs (FTA-SCMNPs) on Fe^{3+} sensing was confirmed using fluorescence titration method. FTA-encapsulated functionalized SCMNPs (FTA-NH_2-SCMNPs and FTA-SO_3H-SCMNPs) were synthesized to demonstrate surface charge effect of nanoparticles on Fe^{3+} fluorescence sensing. The sensing ability of Fe^{3+} followed in this order: FTA-SO_3H-SCMNPs> FTA-SCMNPs> FTA-NH_2-SCMNPs, which rules that particles with stronger negative charge have better sensing abilities. Moreover, linear correlation between quenching intensity and lower concentration of Fe^{3+} was accord to Stern-Volmer equation in FTA-SCMNPs and FTA-SO_3H-SCMNPs. FTA-SO_3H-SCMNPs showed good selectivity of Fe^{3+} detection. Because of the charge effect of functionalized SCMNPs on dye-doped Fe^{3+} sensing system, these kinds of nanoparticles offered possibilities to construct sensing ability-enhanced fluorescence-quenching sensors by tuning surface charge.

Introduction

Fluorescence chemosensors has developed rapidly because of their ability to provide a simple and economical method for online monitoring.[1-12] The samples need not to be pre-treated and their fluorescence emission would change obviously in the form of fluorescence quenching,[13] enhancement[14] or shift[15] during sensing process. Over the past decades, many molecular units have been successfully synthesis and design as fluorescence sensing materials.[3, 6, 16-18] As one of the common metal irons involved in biological processes, iron plays very important part in cell activity regulation and muscle contraction. Thus, many fluorescent iron probes have been proposed.[5, 16, 19] However, most of the organic molecular iron sensors have a poor water-solubility and biocompatibility, which would cause some limitations for biological system. Moreover, some metal ions induced a spirolactam ring-opening hydrolysis of iron sensing molecular and give rise to the influence of emission stability during sensing process.

For overcoming these problems, the design of multicomponent chemosensors using nanostructures as an effective platform is increasingly fascinating.[20, 21] Recently, researchers built a variety of chemosensors with both organic and inorganic parts，which integrate multiple functions or properties into nanostructures.[22-26] Most of nanostrcutures including nanoparticles,[27] nanowires,[28] nanotubes,[29] and nanosheets[30] have been introduced into sensing systems because of their unique quantum size effect, interface, and dielectric confinement. For example, Wang and co-workers incorporated silica film with conjugated polymer for Fe^{3+} detection in both organic and aqueous media.[11] The film sensor with silica-based nanostructure was prepared with surface modification method, which exhibits good selectivity and low detection limits. Mou and co-workers prepared mesoporous silica nanoparticles (MSNs) with surface charge tuneable character for fluorescent ratiometric pH imaging.[31] Li and co-workers synthesized a DNA–graphene oxide(GO)-Fenton hybrid sheet with no-conjugated self-assembly method for highly selective and sensitive fluorescence detection of HO • and Fe^{2+}.[32] Similar assembly process of single-walled carbon nanotubes (SWNTs) and single-stranded DNA was reported to develop a class of fluorescent biosensors which are able to recognize biomolecular interactions.[33] Besides these, quantum dots and gold nanoparticles are also supposed to be good inorganic parts to incorporate organic moieties for the construction of multicomponent chemosensors. [34, 35]

Among the available multicomponent sensing system, luminescent chemosensors based on silica-cross linked micellar nanoparticles (SCMNPs) have been attracted increasing attention in biological sensing. [36-40] Because of their extended PEO chains, high surface mobility and PPO hydrophobic core, SCMNPs have been widely studied to incorporate conjugated organic moieties[41] for improving water dispersity and biocompatibility. Moreover, ultrasmall space of its hydrophobic core encapsulated with organic sensing moieties lead to unique fluorescence properties and complex photophysic processes, which result in higher selectivity or sensitivity in sensing system.[42, 43]

Since the first time synthesis of SCMNPs,[38] various luminescent nanoparticles based on SCMNPs have been prepared using dye-doped method for constructing water-soluble sensing system.[37, 40, 43-45] Energy transfer processes have been successfully introduced into dye-doped SCMNPs by Prodi and co-workers[46] for reversible photoswiching[47] and fluorescence signal amplifying.[43] Our previous work[45] focused on the design of dye-doped SCMNPs for energy transfer-based porphyrin sensing and white-light emitting. Most recently, we make effort on further investigation of electron transfer-based dye-doped SCMNPs to build high selectivity Fe^{3+} sensing system.[48]

The typical method to achieve functionalized silica nanoparticles is to modify surfactant, silica shell, or both surfactant and silica shell.[38, 49] The method of encapsulating host molecules in SCMNPs core have been widely studied for water-soluble fluorescence sensing material design. However, sensing ability tuning via dye-doped SCMNPs shell modification has reported rarely. The design of dye-doped sensing system with good sensing ability is crucial for medical and biological application.

In this study, a novel strategy for improving Fe^{3+} sensing ability has been demonstrated by tuning electron transfer process of dye-doped SCMNPs sensing system. We modified SCMNPs shell with different moieties, which induced different surface charge to achieve electron transfer-enhanced sensing process. By encapsulating a Donor-Acceptor (D-A) dye 4-formacyl-triphenylamine (FTA), FTA-SCMNPs exhibit a fluorescence-enhanced emission and favour Fe^{3+} sensing in aqueous media. In FTA-SO_3H-SCMNPs and FTA-NH_2-SCMNPs, sensing ability of Fe^{3+} influenced by the surface charge of nanoparticles. FTA-SO_3H-SCMNPs performed good selectivity detection of Fe^{3+}. It is indicates that the negative charged FTA-SO_3H-SCMNPs facilitate electron transfer process, which can be used for Fe^{3+} quantitative determination in water.

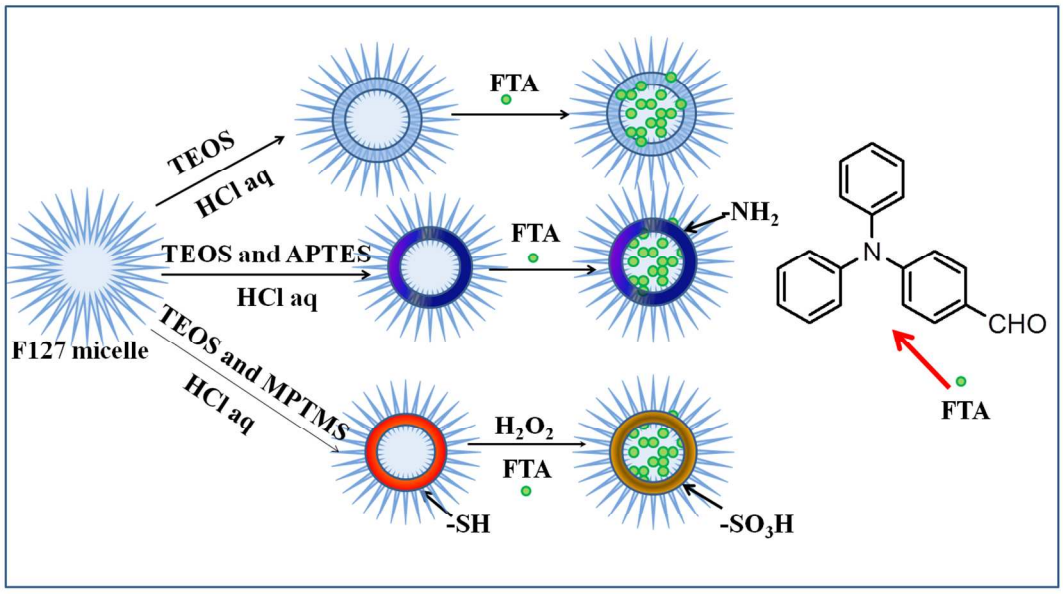

Scheme 1 Synthesis route of FTA-SCMNPs and functionalized FTA-SCMNPs

Experimental Section

Materials

Trimethoxysilylpropanethiol (MPTMS), (3-aminopropyl) triethoxysilane (APTES), Pluronic nonionic surfactant F127, diethoxydimethylsilane ($Me_2Si(OEt)_2$, DEDMS) and tetraethylorthosilicate (TEOS, 99.99%) were purchased from Sigma-Adrich. Ethanol (CH_3CH_2OH, 95%), Acetic acid (CH_3COOH, ≥ 99.5%), Triphenylamine (TPA, ≥98%), hydrochloric acid (fuming, ≥ 37%), anhydrous Ferricchloride ($FeCl_3$, ≥97%) and acetonitrile (CH_3CN, ≥ 97%) were purchased from Aladdin. 4-Aminoantipyrine (98%) was purchased from Alfa Aesar. The dialysis tubing (M_w cutoff: 8000–14, 400) was purchased from Aldrich. All reagents and solvents were used without further purification. Deionised water was used in our experiment (Resistivity ≥ 18.2 MΩ).

Synthesis of FTA

The synthetic detail of FTA was described in the supporting information. FTA (4-formacyl-triphenylamine) was obtained via a Vilsmeier reaction.[50] Mass spectrum (MS) data of FTA showed in supporting information.

Synthesis of the FTA-SCMNPs and Functionalized FTA-SCMNPs

First, An acidic aqueous solution of F127 (0.6 g of F127 in 9.4 g of 0.85 M HCl solution) was added to a glass vial. 1 g of TEOS was added. After an additional 0.5 h of stirring, 0.06 g of DEDMS was added. The as-made product was dialyzed by deionised water to remove HCl and get silica cross-linked micellar nanoparticles (SCMNPs).[37, 38, 43-45] 0.1ml FTA was dissolved in acetonitrile solvent to get its solution with concentration of about 1×10^{-4} M. A specific amount of the dye solution was put into a vial and the solvents were completely removed in a vacuum oven at 40 °C to prevent the organic solvent from destroying the micelles of F127. Then, 2ml SCMNPs suspension was added in to the vial, and after 0.5 h of stirring, the

FTA-SCMNPs were treated with dialysis using a dialysis tube (cutoff: 8,000-14,400) and a 0.22μm Teflon filter to ensure that all the low molecular (such as HCl and silane) and large solid impurities would be removed from the product. [38, 45]

Functionalized dye-SCMNPs were prepared by using suitable functional silanes as co-precursor with TEOS. The silane was combined with silica precursor (e.g., TEOS) first, and then the functionalized nanoparticles were synthesized by following the typical procedure for non-functionalized particles.

Synthesis of amino Functionalized dye-SCMNPs (FTA-NH_2-SCMNPs): A typical preparation for the synthesis of amino functionalized nanoparticles is as follows: 0.6 g of F127 was dissolved in 9.4 g of HCl (0.85 M) aqueous solution with stirring. Then a mixture of 0.67g of TEOS and 0.13 g of (3-aminopropyl) triethoxysilane (APTES) was added to the homogeneous solution with stirring. 40 min later, 0.2 g of TEOS was added. After stirring for 20 minutes, 0.08 g of DEDMS was added. The solution was stirred for another 30 minutes or longer.

Synthesis of sulfonic functionalized dye-SCMNPs (FTA-SO_3H-SCMNPs) was based on thiol-functionalized SCMNPs (MPTMS-SCMNPs) which consequently oxidized to sulfonic-SCMNPs (SO_3H-SCMNPs). The encapsulation process is similar to the synthesis process of FTA-NH_2-SCMNPs (Scheme 1).

Stability of FTA-SCMNPs

The leakage of the FTA from SCMNPs was tested using a dialysis method.[45] After a dialysis process for 1 h, the solutions inside and outside of the dialysis tube were both analyzed with inductively coupled plasma (ICP) and fluorescence emission spectra. The stability has been investigated by the comparison as-maded samples and samples that synthesized 90 days ago.

Characterization

Transmission electron microscopy (TEM) was carried out using FEI Tecnal G2 F20 s-twin D573 operated at 200 kV. The sample for TEM was prepared by directly placing a small drop of the nanoparticles suspension on a carbon-coated TEM grid. Inductively coupled plasma (ICP) analyses were carried out on a Perkin-Elmer Optima 3300DV ICP instrument. The particle size of SCMNPs was measured by a Malvern Zetasizer Nano-S instrument using Dynamic Light Scattering (DLS) principles with a HeNe laser (633 nm). Zeta potential measurements were conducted using a Zetasizer NanoZS (Malvern Instruments). The fluorescence emission spectra of the samples were recorded on a HORIBA Instrument FluoroMax - Compact spectrofluorometer. ^{1}H NMR of FTA was obtained on an Avance III instrument (Brucker, 300 MHz). Mass spectrometry (MS) of FTA was carried out on a Brucker Instrument (Agilent1290-micr OTOF Q II).

Result and discussion

Based on our most recently report[48] of Fe^{3+} sensor, in this paper, further exploration of dye-doped SCMNPs sensing system have been made to induce FTA (4-formacyl-triphenylamine) as a intramolecular charge transfer D-A dye to SCMNPs and functionalized SCMNPs for sensing ability enhancement of Fe^{3+}. The advantage of FTA-SCMNPs as follows: First, FTA-SCMNPs exhibit fluorescence-enhanced effect to inhibit excited state emission quenching of free FTA in aqueous media, which result in a applicable design of a water-soluble dye-doped SCMNPs Fe^{3+} sensing systems. Moreover, Triphenylamine is more easily than phenothiazine moiety to obtain charge transfer and electron transfer process, thus FTA-SCMNPs obtained better sensing ability of Fe^{3+} than EDDP-SCMNPs in aqueous media.[51, 52] The synthesis of aldehyde-derived Triphenylamine(FTA) was easier than Triphenylamine-based schiff base and the investigation of FTA-SCMNPs on electron transfer-based Fe^{3+} sensing was rarely reported. Furthermore, we extend our study to functionalized shell by modifying positive-charged amino-group (-NH_2) and negative-charged Sulfonic acid group (-SO_3H) onto the surface of SCMNPs. Our thought is to enhance Fe^{3+} sensing ability by tuning surface charge of SCMNPs shell.

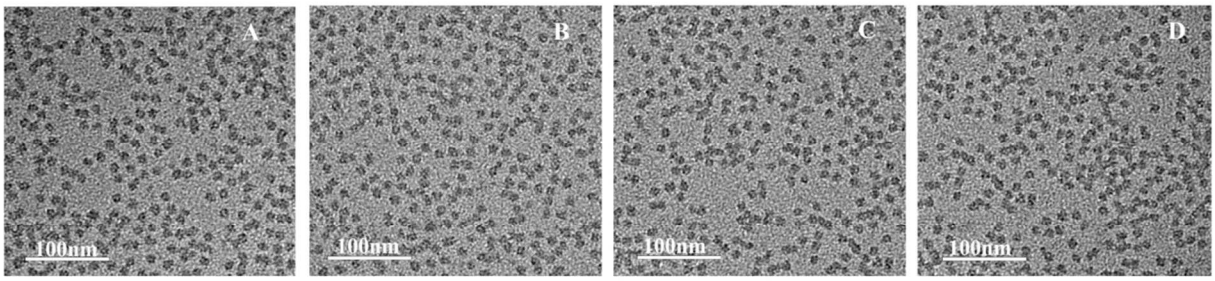

Fig.1 TEM image of (A) FTA-SCMNPs, (B) FTA-NH_2-SCMNPs, (C) FTA- SO_3H-SCMNPs (zeta potential -17.6 mV) and (D) FTA- SO_3H-SCMNPs (zeta potential -22.47 mV)

Morphology of FTA-SCMNPs and functionalized FTA-SCMNPs

The synthesis route of FTA encapsulated in SCMNPs (FTA-SCMNPs), NH_2-SCMNPs (FTA-NH_2-SCMNPs) and SO_3H-SCMNPs (FTA-SO_3H-SCMNPs) showed in Scheme 1. Among them, SO_3H-SCMNPs synthesized during oxidation process from SH-SCMNPs by H_2O_2. All the products suggested no dissolved silica shell and no leakage of FTA during ICP and fluorescence spectra techniques, which indicates steady fluorescent particles have been prepared.

As is shown in Figure 1A, 1B and 1C, monodispersed nanoparticles obtained with SCMNPs, NH_2-SCMNPs and SO_3H-SCMNPs as silica shell. TEM image indicates that three kinds of surface charged nanoparticles showed similar morphology and size, which showed particles diameters are about 13nm (Fig. 1).

DLS data showed similar size distribution of three kinds of nanoparticles, which indicates that the hydrodynamic diameters of nanoparticles are about 20-25nm (Fig. 2).

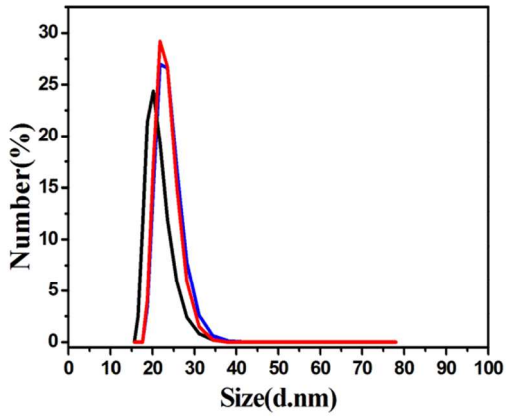

Fig.2 DLS of FTA-SCMNPs (black), FTA-NH_2-SCMNPs (red) and FTA- SO_3H-SCMNPs (blue)

Although the sizes of DLS and TEM are not the same, the DLS showed no contrast to the TEM study. Because of the outer shell PEO chains extended in aqueous media when tested by DLS techniques, the size of three kinds of nanoparticle showed larger size in DLS than that showed in TEM.[38, 53] The size and morphology are consistent with our recent work,[48] which indicates that treatment of condensation and oxidation could not change the morphology and dispersity of nanoparticles.

The stability of three kinds of nanoparticles also has been verified by PDI value, TEM and DLS after keeping samples for at least 3 months. We visually evaluated the three samples synthesized 3 months ago and found that no precipitation and cloudiness could be detected. The TEM image and DLS data also showed similar results to freshly-made samples. The PDI values of the three samples are all about 0.09 after being kept at room temperature for 3 months, which suggested good monodispersity and stability of three samples in aqueous media.[45]

We also investigated the surface charge effect of nanopartcles stability. The zeta potentials of FTA-SCMNPs, FTA-NH_2-SCMNPs and FTA-SO_3H-SCMNPs have been shown in Table 1. The positively charged ($\zeta_{FTA\text{-}NH_2\text{-}SCMNPs}$ 1.7mV) and negatively charged ($\zeta_{FTA\text{-}SCMNPs}$ -10.3 mV and $\zeta_{FTA\text{-}SO_3H\text{-}SCMNPs}$ mV) nanoparticles showed no precipitation and good monodispersity after being kept for 3 months, which suggested that the repulsion between particles[54] and the contribution of PEG outer nanoaprticles shell[55-57] resulted in good stability of SCMNPs suspension. Thus, low negatively charged and positively charged zeta potential would not cause aggregation in FTA- SCMNPs and functionalized FTA-SCMNPs sensing system.

Table 1 Zeta potential (ζ) and limit of detection (LOD) of FTA-NH_2-SCMNPs (A), EDDP-SCMNPs (B), FTA-SCMNPs (C), and FTA-SO_3H-SCMNPs (D and E)

	A	B	C	D	E
ζ/ mV	1.7	-9.4	-10.3	-17.6	-22.5
LOD/ ppm	17	5.3	4	1.3	1

Sensing ability of FTA-SCMNPs and functionalized FTA-SCMNPs

To demonstrate the influence of nanoparticles surface charge on Fe^{3+} sensing, we designed two luminescent nanoparticles functionalized with -NH_2 and -SO_3H for fluorescence quenching investigation. Because the twist intramolecular charge transfer (TICT) and photoinduced charge transfer (ICT) of FTA[50, 58, 59] may both occur in the core of SCMNPs, which would facilitate electron transfer process in Fe^{3+} sensing, free FTA showed weak fluorescence, while FTA-SCMNPs showed a enhanced fluorescence. (The reason and detailed discussion of this phenomenon will report in our next paper.) Fig.3 showed that the strong emission of FTA-SCMNPs, which indicates that the weak fluorescence dyes are applicable to the design of SCMNPs-based fluorescence quenching sensor. Thus, we use FTA-SCMNPs for constructing Fe^{3+} fluorescence probe in aqueous media to propose the aldehyde-derived D-A dye of Fe^{3+} fluorescence quenching sensor design by SCMNPs system. As is shown in Figure 4(A), an increasing amount of Fe^{3+} gradually quenched FTA-SCMNPs emission with a detection limit of 4ppm. With the addition of Fe^{3+} increasing continually, FTA-SCMNPs fluorescence quenched to 10% of its original intensity. Table 1(A) and (B) showed that FTA-SCMNPs exhibit ζ -10.3mV and limit of detection(LOD) 4ppm, which got a lower zeta potential and a lower limit detection of Fe^{3+} than EDDP-SCMNPs (ζ -9.4mV and LOD 5.3ppm). From the observation of fluorescence quenching spectra, we find that FTA emission decreased without shift or other shape change after adding Fe^{3+}, which indicates that the electron-accepting agent facilitate TICT and ICT emission quenching[50, 60] in electron transfer sensing process.[48] The quenching of FTA-SCMNPs ascribe to electron transfer process from FTA in the core to Fe^{3+} on the shell,[48] which was consistent with our previous work.

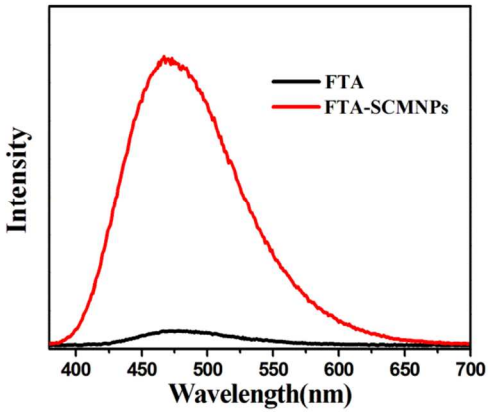

Fig.3 Fluorescence enhancement of FTA-SCMNPs (red: FTA-SCMNPs, black: FTA in H_2O/CH_3CN=20/1)

To get more evidence of electron transfer-based Fe^{3+} sensing process, we functionalized SCMNPs shell with -NH_2 and -SO_3H for surface charge tuning of Fe^{3+} sensing system. As is shown in Table 1(A), FTA-NH_2-SCMNPs got a positive charged surface and a high LOD of 17ppm. Fig. 4(B) shows that fluorescence emission spectra of FTA-NH_2-SCMNPs are broader than that of FTA-SCMNPs, which result from the influence of NH_2 on the shell. Compare to the detection limit of FTA-SCMNPs, FTA-NH_2-SCMNPs have almost no quenching by Fe^{3+} at low concentration levels (from 4ppm to about 15ppm).

Fig. 4(C) shows surface negative charged FTA-SO_3H-SCMNPs (ζ -22.5 mV) quenched linearly by adding an increasing amount of Fe^{3+} with low detection limit of 1ppm. This value is lower than detection limit of FTA-NH_2-SCMNPs (30ppm) and FTA-SCMNPs (4ppm), which is consistent with our deduction. More evidence of charge effect on sensing ability was verified using another sample of FTA-SO_3H-SCMNPs (ζ -17.6 mV). As is shown in Fig.4(D), the LOD of FTA-SO_3H-SCMNPs (ζ -17.6 mV) is 1.25ppm, which is higher than the LOD of FTA-SO_3H-SCMNPs(ζ -22.5 mV). This lower sensing ability of Fe^{3+} can be ascribing to the lower charge of the sensor.

Considering the zeta potential and the sensing ability in Table 1, we can find that the detection limit of Fe^{3+} is in the sequence: FTA-NH_2-SCMNPs> FTA-SCMNPs> FTA-SO_3H-SCMNPs, which is ascribe to the zeta potential sequence. As we discussed above, this sensing system based on ET process[48] and ET process is influenced by electron-accepting ability and the distance between electron donor and acceptor,[48] thus, the surface charge of nanoparticles plays dominant role in absorbing Fe^{3+} on silica shell which would result in closer distance between Fe^{3+} and FTA in the core. The different zeta potential of sensing system could cause different ability of Fe^{3+} detection. Therefore, the amino group and protonated silanol species[10, 54] on shell would enhance the repulsion between Fe^{3+} and nanoparticles, which cause an inhibition of ET process. On the other hand, the negative charge of -SO_3H on surface shell would enhance the electronic attraction between SO_3H-SCMNPs shell and Fe^{3+}, thus, Fe^{3+} can easily absorb onto silica shell for narrowing down the distance between electronic donor and acceptor. In other word, negative surface charge would facilitate charge transfer from FTA to Fe^{3+} in this sensing system[61].

We also give the relationship of Fe^{3+} concentration and fluorescence intensity in Fig. 4(E). The log curve of four sensing systems indicates that FTA-SCMNPs and FTA-SO_3H-SCMNPs showed better Fe^{3+} sensing ability than FTA-NH_2-SCMNPs. When above sensing systems contains high concentration of Fe^{3+} (>30 ppm), surface charge of all the samples changed by Fe^{3+}, and thus, the fluorescence of each sensing system indicates no linear correlation with Fe^{3+} concentration. However, when the concentration of Fe^{3+} (<25 ppm) is low, we can find that obvious quenching of surface negative-charged FTA-SCMNPs and FTA-SO_3H-SCMNPs were showed in Fig.4(E) and also their quenching intensity and concentration linear relationship are better than the positive charged FTA-NH_2-SCMNPs(Fig.5). Therefore, surface charge effect of the four sensing systems plays predominant role in tuning the detection limits of Fe^{3+} in aqueous media.

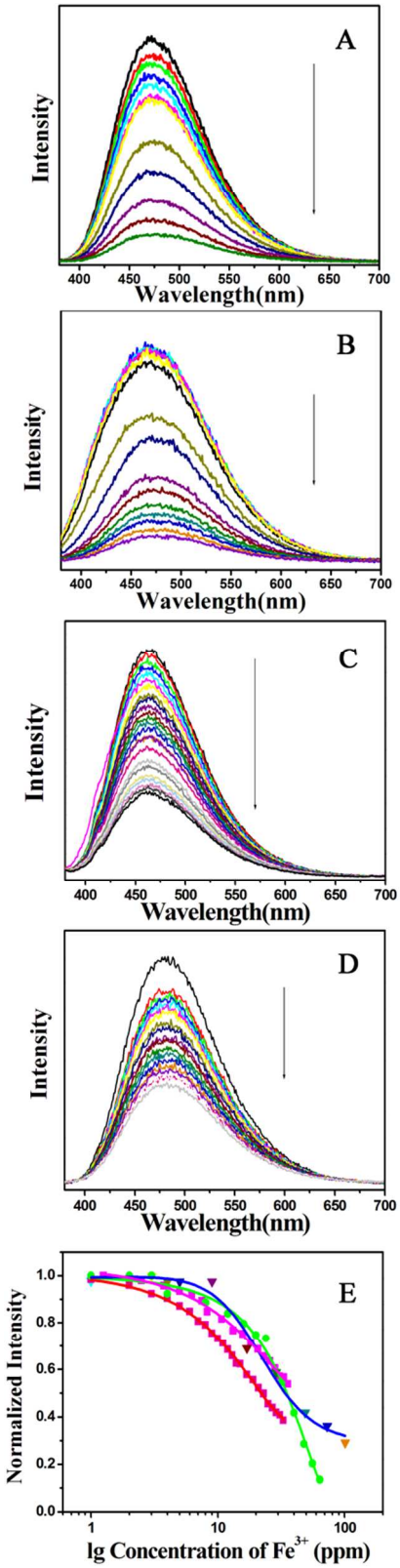

Fig.4 Fluorescence emission of (A)FTA-SCMNPs, (B) FTA-NH_2-SCMNPs (C) FTA-SO_3H-SCMNPs (-22.5mV) and (D) FTA-SO_3H-SCMNPs (-17.6mV) with an increasing amount of Fe^{3+} (excitation 377nm);(E) Relative fluorescence intensity of four type nanoparticles (green: FTA-SCMNPs, red: FTA-SO_3H-SCMNPs (-22.5mV), blue: FTA-NH_2-SCMNPs and pink: FTA-SO_3H-SCMNPs (-17.6mV)) in Fe^{3+} quenching

The metal ions influence of FTA-SO_3H-SCMNPs has been investigated by fluorescence emission, which showed a good selectivity detection of Fe^{3+} (Fig.S2). We found that almost no fluorescence quenching could be detected after the addition of Cu^{2+}, Fe^{2+}, Ni^{2+}, Co^{2+}, Hg^{2+}, Zn^{2+}, etc, while the same concentration of Fe^{3+} could cause an obvious fluorescence quenching of FTA-SO_3H-SCMNPs emission. Therefore, the negatively charged FTA-SO_3H-SCMNPs showed both good detection selectivity and sensing ability of Fe^{3+} in aqueous media.

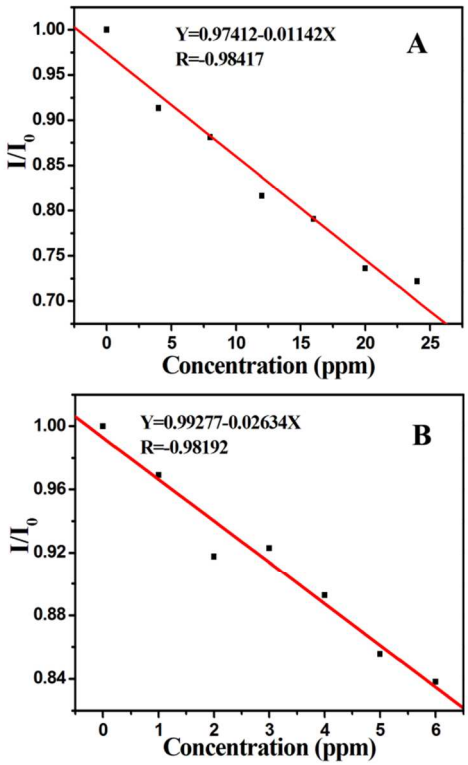

Fig.5 Relative fluorescence emission intensity (I/I_0) of (A) FTA-SCMNPs and (B) FTA-SO_3H-SCMNPs in Fe^{3+} sensing

Linear analysis of Fe^{3+} sensing by FTA-SCMNPs and FTA-SO_3H -SCMNPs

Based on the above analysis, the Fe^{3+} detection limit is in the order of FTA-SO_3H-SCMNPs< FTA-SCMNPs< FTA-NH_2-SCMNPs. Subsequently, we further investigated fluorescence quenching by Fe^{3+} using Stern–Volmer equation:

$$F_0/F = 1 + K_{SV}[Q],$$

where F_0 and F are the fluorescence intensities in the absence and presence of quencher, K_{SV} is the Stern-Volmer quenching constant, and Q is the concentration of the quencher. [10, 61-63] The concentration of quenching can be calculating by fluorescence intensity. From the observation of quenching processes, there are nonlinear relationship between relatively fluorescence intensity (I/I_0) and high Fe^{3+} concentration (> 30ppm) in three sensing systems. However, at low (below 30 ppm) concentration, I/I_0 of FTA-SCMNPs and FTA-SO_3H-SCMNPs showed linear correlation separately.

As shown in Fig. 5, both fluorescence intensity of FTA-SCMNPs and FTA-SO_3H-SCMNPs possess good linear correlation with Fe^{3+} concentration. The corresponding linear regression equations, where Y is the relative fluorescence intensity (I/I_0) and X is the concentration of Fe^{3+}, and the correlation coefficients (R) are presented in Figure 6. Thus, one can choose the equation to quantify the concentration of Fe^{3+}.

Conclusions

In summary, the surface charge effect of ET-based Fe^{3+} sensing system have been investigated, and the sensitivity of Fe^{3+} detection is accord with the negative charge density of nanoparticles. The aldehyde-derived dye-doped SCMNPs Fe^{3+} sensing systems have been proposed by introducing D-A molecule FTA into silica cross-linked micellar nanoparticles. The FTA-doped SCMNPs sensing system possesses good selectivity detection of Fe^{3+} in aqueous media. The twist intramolecular charge transfer (TICT) and photoinduced charge transfer (ICT) of FTA exhibit an easier ET process than phenothiazine moieties in our latest report, which give rise to a lower detection limit of Fe^{3+}. Moreover, we successfully decreased detection limits by tuning surface charge of functionalized SCMNPs shell. Consequently, linear relationship between quenching intensity and Fe^{3+} concentration correlated with Stern-Volmer equation, which would achieve a quantitative Fe^{3+} sensing at ppm level in aqueous media.

Acknowledgements

This work was supported by the National Natural Science Foundation of China (Nos. 21371067, 21373095 and 21171064)

Notes and references

[a] *State Key Laboratory of Inorganic Synthesis and Preparative Chemistry, College of Chemistry, Jilin University, Changchun 130012, Tel: +86-431-85168602; E-mail: huoqisheng@jlu.edu.cn*
[b] *State Key Laboratory of Supramolecular Structure and Materials, College of Chemistry, Jilin University, Changchun 130012, China. Tel: +86-431-5168484*

† Electronic Supplementary Information (ESI) available: The Mass Spectroscopy of FTA is shown in supporting information. See DOI: 10.1039/b000000x/

1. Y. Zhang, M. Wang, Y. G. Zheng, H. Tan, B. Y. W. Hsu, Z. C. Yang, S. Y. Wong, A. Y. C. Chang, M. Choolani, X. Li and J. Wang, *Chem. Mater.*, 2013, **25**, 2976-2985.
2. Y. F. Ma, Y. Li, S. J. Ma and X. H. Zhong, *Journal of Materials Chemistry B*, 2014, **2**, 5043-5051.
3. J. Du, M. Hu, J. Fan and X. Peng, *Chem. Soc. Rev.*, 2012, **41**, 4511-4535.
4. R. Wen Xiu, H. Jiyou, T. Pradhan, L. Ja-Yun, L. Jae Hong, L. Jaehun, K. Jong-Hoon and K. Jong Seung, *Biomaterials*, 2014, **35**, 4157-4167.
5. S. K. Sahoo, D. Sharma, R. K. Bera, G. Crisponi and J. F. Callan, *Chem. Soc. Rev.*, 2012, **41**, 7195-7227.
6. L. Zhao, Y. Chu, C. He and C. Duan, *Chem. Commun.*, 2014, **50**, 3467-3469.
7. N. R. Chereddy, S. Thennarasu and A. B. Mandal, *Dalton Transactions*, 2012, **41**, 11753-11759.
8. P. Li, L. Fang, H. Zhou, W. Zhang, X. Wang, N. Li, H. Zhong and B. Tang, *Chemistry – A European Journal*, 2011, **17**, 10520-10523.
9. T. Hirayama, K. Okuda and H. Nagasawa, *Chemical Science*, 2013, **4**, 1250-1256.

10. J. Han, Z. Zhou, X. Bu, S. Zhu, H. Zhang, H. Sun and B. Yang, *Analyst*, 2013, **138**, 3402-3408.
11. X. Wu, B. Xu, H. Tong and L. Wang, *Macromolecules*, 2010, **43**, 8917-8923.
12. D. Genovese, E. Rampazzo, S. Bonacchi, M. Montalti, N. Zaccheroni and L. Prodi, *Nanoscale*, 2014, **6**, 3022-3036.
13. Q. Meng, W. Su, C. He and C. Duan, *Talanta*, 2012, **97**, 456-461.
14. M. H. Lee, T. V. Giap, S. H. Kim, Y. H. Lee, C. Kang and J. S. Kim, *Chem. Commun.*, 2010, **46**, 1407-1409.
15. W. Lin, L. Long, L. Yuan, Z. Cao, B. Chen and W. Tan, *Org. Lett.*, 2008, **10**, 5577-5580.
16. Y. Yang, Q. Zhao, W. Feng and F. Li, *Chem. Rev.*, 2012, **113**, 192-270.
17. X.-L. Shi, G.-J. Mao, X.-B. Zhang, H.-W. Liu, Y.-J. Gong, Y.-X. Wu, L.-Y. Zhou, J. Zhang and W. Tan, *Talanta*, 2014, **130**, 356-362.
18. L. Qiu, T. Zhang, J. Jiang, C. Wu, G. Zhu, M. You, X. Chen, L. Zhang, C. Cui, R. Yu and W. Tan, *J. Am. Chem. Soc.*, 2014, **136**, 13090-13093.
19. E. L. Que, D. W. Domaille and C. J. Chang, *Chem. Rev.*, 2008, **108**, 1517-1549.
20. L. Z. Zhao, J. J. Peng, M. Chen, Y. Liu, L. M. Yao, W. Feng and F. Y. Li, *Acs Applied Materials & Interfaces*, 2014, **6**, 11190-11197.
21. K. Y. Liu, Y. Wen, T. Shi, Y. Li, F. Y. Li, Y. L. Zhao, C. H. Huang and T. Yi, *Chem. Commun.*, 2014, **50**, 9141-9144.
22. S. Palantavida, R. Tang, G. P. Sudlow, W. J. Akers, S. Achilefu and I. Sokolov, *Journal of Materials Chemistry B*, 2014, **2**, 3107-3114.
23. X. He, H. Nie, K. Wang, W. Tan, X. Wu and P. Zhang, *Anal. Chem.*, 2008, **80**, 9597-9603.
24. Z. Zhao, H. Meng, N. Wang, M. J. Donovan, T. Fu, M. You, Z. Chen, X. Zhang and W. Tan, *Angew. Chem. Int. Ed.*, 2013, **52**, 7487-7491.
25. W. Zhong, *Anal. Bioanal. Chem.*, 2009, **394**, 47-59.
26. L. Bau, P. Tecilla and F. Mancin, *Nanoscale*, 2011, **3**, 121-133.
27. S. Jiang, K. Y. Win, S. Liu, C. P. Teng, Y. Zheng and M.-Y. Han, *Nanoscale*, 2013, **5**, 3127-3148.
28. in *Nanotubes and Nanowires (2)*, The Royal Society of Chemistry, 2011, pp. 343-530.
29. R. K. Joshi and J. J. Schneider, *Chem. Soc. Rev.*, 2012, **41**, 5285-5312.
30. S. Bai and X. Shen, *RSC Advances*, 2012, **2**, 64-98.
31. Y.-P. Chen, H.-A. Chen, Y. Hung, F.-C. Chien, P. Chen and C.-Y. Mou, *RSC Advances*, 2012, **2**, 968-973.
32. W. T. Huang, W. Y. Xie, Y. Shi, H. Q. Luo and N. B. Li, *J. Mater. Chem.*, 2012, **22**, 1477-1481.
33. R. Yang, Z. Tang, J. Yan, H. Kang, Y. Kim, Z. Zhu and W. Tan, *Anal. Chem.*, 2008, **80**, 7408-7413.
34. T. Chen, H. Yu, N. E. Yang, M. D. Wang, C. D. Ding and J. J. Fu, *Journal of Materials Chemistry B*, 2014, **2**, 4979-4982.
35. H. L. Yang, S. W. Li, X. Y. Zhang, X. Y. Wang and J. T. Ma, *Journal of Materials Chemistry A*, 2014, **2**, 12060-12067.
36. M. Montalti, E. Rampazzo, N. Zaccheroni and L. Prodi, *New J. Chem.*, 2013, **37**, 28-34.
37. S. Bonacchi, D. Genovese, R. Juris, M. Montalti, L. Prodi, E. Rampazzo and N. Zaccheroni, *Angew. Chem. Int. Ed.*, 2011, **50**, 4056-4066.
38. Q. Huo, J. Liu, L.-Q. Wang, Y. Jiang, T. N. Lambert and E. Fang, *J. Am. Chem. Soc.*, 2006, **128**, 6447-6453.
39. Y. Zhang, M. Wang, Y.-g. Zheng, H. Tan, B. Y.-w. Hsu, Z.-c. Yang, S. Y. Wong, A. Y.-c. Chang, M. Choolani, X. Li and J. Wang, *Chem. Mater.*, 2013, **25**, 2976-2985.
40. M. Yu, S. Karmakar, J. Yang, H. Zhang, Y. Yang, P. Thorn and C. Yu, *Chem. Commun.*, 2014, **50**, 1527-1529.
41. H. Tan, Y. Zhang, M. Wang, Z. Zhang, X. Zhang, A. M. Yong, S. Y. Wong, A. Y.-c. Chang, Z.-K. Chen, X. Li, M. Choolani and J. Wang, *Biomaterials*, 2012, **33**, 237-246.
42. E. Rampazzo, S. Bonacchi, D. Genovese, R. Juris, M. Montalti, V. Paterlini, N. Zaccheroni, C. Dumas-Verdes, G. Clavier, R. Méallet-Renault and L. Prodi, *The Journal of Physical Chemistry C*, 2014, **118**, 9261-9267.
43. E. Rampazzo, S. Bonacchi, D. Genovese, R. Juris, M. Sgarzi, M. Montalti, L. Prodi, N. Zaccheroni, G. Tomaselli, S. Gentile, C. Satriano and E. Rizzarelli, *Chemistry – A European Journal*, 2011, **17**, 13429-13432.
44. D. Genovese, S. Bonacchi, R. Juris, M. Montalti, L. Prodi, E. Rampazzo and N. Zaccheroni, *Angew. Chem. Int. Ed.*, 2013, **52**, 5965-5968.
45. F. Gai, T. Zhou, L. Zhang, X. Li, W. Hou, X. Yang, Y. Li, X. Zhao, D. Xu, Y. Liu and Q. Huo, *Nanoscale*, 2012, **4**, 6041-6049.
46. E. Rampazzo, S. Bonacchi, R. Juris, M. Montalti, D. Genovese, N. Zaccheroni, L. Prodi, D. C. Rambaldi, A. Zattoni and P. Reschiglian, *The Journal of Physical Chemistry B*, 2010, **114**, 14605-14613.
47. D. Genovese, M. Montalti, L. Prodi, E. Rampazzo, N. Zaccheroni, O. Tosic, K. Altenhoner, F. May and J. Mattay, *Chem. Commun.*, 2011, **47**, 10975-10977.
48. F. Gai, X. Li, T. Zhou, X. Zhao, D. Lu, Y. Liu and Q. Huo, *Journal of Materials Chemistry B*, 2014, **2**, 6306-6312.
49. L.-L. Li, H. Sun, C.-J. Fang, Q. Yuan, L.-D. Sun and C.-H. Yan, *Chem. Mater.*, 2009, **21**, 4589-4597.
50. Y. Mo, F. Bai, D. Zhang, Z. Wang and D. Zhu, *Science in China,Ser.B*, 1996, 255-259.
51. W. Lin, L. Yuan, J. Feng and X. Cao, *Eur. J. Org. Chem.*, 2008, **2008**, 2689-2692.
52. P. Wu, J. Wang, C. He, X. Zhang, Y. Wang, T. Liu and C. Duan, *Adv. Funct. Mater.*, 2012, **22**, 1698-1703.
53. Y.-M. Lam, N. Grigorieff and G. Goldbeck-Wood, *PCCP*, 1999, **1**, 3331-3334.
54. F. Chi, B. Guan, B. Yang, Y. Liu and Q. Huo, *Langmuir*, 2010, **26**, 11421-11426.
55. J. Lin, J. Zhu, T. Chen, S. Lin, C. Cai, L. Zhang, Y. Zhuang and X.-S. Wang, *Biomaterials*, 2009, **30**, 108-117.
56. Y. Wang, C.-Y. Ke, C. Weijie Beh, S.-Q. Liu, S.-H. Goh and Y.-Y. Yang, *Biomaterials*, 2007, **28**, 5358-5368.
57. S. Zanarini, E. Rampazzo, S. Bonacchi, R. Juris, M. Marcaccio, M. Montalti, F. Paolucci and L. Prodi, *J. Am. Chem. Soc.*, 2009, **131**, 14208-14209.
58. Y. H. Pang, S. M. Shuang, M. S. Wong, Z. H. Li and C. Dong, *J. Photochem. Photobiol. A: Chem.*, 2005, **170**, 15-19.
59. Y. Tian, C. Y. Chen, Y. J. Cheng, A. C. Young, N. M. Tucker and A. K. Y. Jen, *Adv. Funct. Mater.*, 2007, **17**, 1691-1697.
60. L. Bian, G. Sun, Y. Sun and W. Tang, *J. Phys. Org. Chem.*, 2012, **25**, 1112-1118.
61. in *Principles of Fluorescence Spectroscopy*, ed. J. Lakowicz, Springer US, 2006, ch. 8, pp. 277-330.
62. B. Valeur, in *Molecular Fluorescence*, Wiley-VCH Verlag GmbH, 2001, pp. 72-124.
63. B. Valeur, in *Molecular Fluorescence*, Wiley-VCH Verlag GmbH, 2001, pp. 273-350.

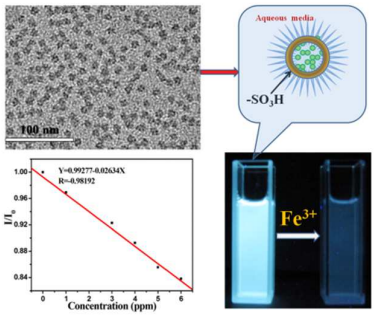

This work demonstrated that a series of electron transfer-based fluorescent chemosensors have been designed by using surface negative-charged silica cross-linked micellar nanoaparticles as scaffolds to encapsulate FTA for improving quantitative Fe^{3+} sensing ability in aqueous media.